Available online at www.sciencedirect.com
SCIENCE DIRECT®
Scripta Materialia 52 (2005) 657–661
Scripta MATERIALIA
www.actamat-journals.com

Effect of strain rate on deformation texture in OFHC copper

A. Bhattacharyya *, D. Rittel [1], G. Ravichandran

Graduate Aeronautics Laboratories, Aeronautics and Mechanical Engineering, California Institute of Technology, 1200 E. California Blvd., Pasadena, CA 91125, USA

Received 31 May 2004; received in revised form 11 November 2004; accepted 18 November 2004
Available online 16 December 2004

Abstract

A strong strain rate dependence on the crystallographic texture of oxygen-free high conductivity copper is observed and reported for the first time. Two shear compression specimens were deformed at widely different strain rates (0.001 s^{-1} and 7000 s^{-1}) to the same strain, and their textures were determined using orientation image microscopy. By comparing the stress–strain curves and the major texture components at the two strain rate levels, it is realized that increase in strain rate causes increase in strain hardening which thereby influences the texture.

Keywords: Shear compression specimen; Orientation image microscopy (OIM); Oxygen-free high conductivity (OFHC) copper; Strain rate; Texture

1. Introduction

Polycrystalline oxygen-free high conductivity (OFHC) copper is one of the most widely studied materials under a variety of deformation paths and over large strains, strain rates and temperatures. As the material deforms, it develops texture due to crystal reorientation. The evolution of the deformation texture with strain at quasi-static strain rates has been analyzed by many researchers to assess the predictive capabilities of crystal-based plasticity models for face-centered cubic (fcc) metals, see e.g. Refs [1,2]. Strong strain rate effects on rolling texture have been previously reported by Leffers [4], and by Leffers and Pedersen for Cu–5%Zn [5]. However, to the best of the authors' knowledge, there has not been a single experiment on OFHC copper aimed at observing the effect of strain rate on deformation texture. This information is much needed in order to check the validity and widen the range of applicability of the current constitutive models, which are mostly strain rate dependent [1,2]. New results for the deformation texture in OFHC copper deformed at high-strain rate are presented here. In order to achieve large deformations at widely different strain rates using single specimen geometry, the newly developed shear compression specimen (SCS) [3] was used throughout the study. The evolution of texture is shown to be rate dependent.

2. Experimental

Two cylindrical cold drawn OFHC copper samples with specifications shown in Table 1 were selected for carrying out compression tests at two widely differing strain rate levels at room temperature. The cylindrical samples were made into SCS by machining two slots at 45° to the drawing direction (along the height), as shown in Fig. 1 [3]. The specimens were tested in the as-received condition. Sample A was compressed quasi-statically at a strain rate ($\dot{\varepsilon}_e$) of 0.001 s^{-1} using a computer controlled servo-hydraulic machine (MTS

* Corresponding author. Tel.: +1 626 395 4748; fax: +1 626 449 6359.
E-mail address: ab03@caltech.edu (A. Bhattacharyya).
[1] Faculty of Mechanical Engineering, Technion, Haifa, Israel.

1359-6462/$ - see front matter © 2004 Acta Materialia Inc. Published by Elsevier Ltd. All rights reserved.
doi:10.1016/j.scriptamat.2004.11.019

Table 1
SCS samples selected for the deformation experiment

Sample	Strain rate (s^{-1})	Initial gage width (w) (mm)	Final gage width (w*) (mm)	Height (h) (mm)
A	0.001	1.27	0.64	29.21
B	7000	2.54	1.27	27.94

Model no. 11019). The total equivalent plastic strain (ε_e) was 0.5. Sample B was compressed similarly at a strain rate ($\dot{\varepsilon}_e$) of 7000 s^{-1} using the split-Hopkinson pressure bar apparatus to the same equivalent strain of 0.5.

The constitutive relations for the SCS copper are given by (from Eqs. (2) and (3) in Rittel et al. [3]),

$$\varepsilon_e = \frac{d}{h}: \quad \dot{\varepsilon}_e = \frac{\dot{d}}{h} \tag{1}$$

$$\sigma_e = 0.85(1 - 0.2\varepsilon_e)\frac{P}{\varphi t} \tag{2}$$

where d is the vertical displacement of the gage section, h is the initial gage height ($= \sqrt{2}$ w), σ_e is equivalent stress, P is the applied load, φ and t are the sample diameter and gage thickness shown in Fig. 1.

After deformation, a thin slice was sectioned midway along the compression direction by including the gage section (Fig. 1), using electro discharge machining (EDM). The sample sections were then mechanically ground and electropolished.

The crystallographic orientation measurements on the sample surfaces were carried out by using orientation imaging microscopy (OIM) [6,7], which employs fully automated (computerized) identification of the back-scattered Kikuchi diffraction patterns and an automated computation of the crystal lattice orientation. The OIM technique has a typical spatial resolution of about 1 μm. The OIM scans in this study covered a maximum area of approximately 1 mm × 1 mm at a time. Scans were recorded at different regions, (Fig. 1(a)–(c)), along the compression direction, for both the samples A and B.

3. Results

After compressing the SCS samples at two different strain rates to the same nominal strain, it was observed by measuring the dimensions that the cylindrical sections containing regions a and c remained undeformed, whereas the gage section containing region b appeared to be sheared. This is in agreement with the report of Rittel et al. [3] of the deformation pattern of the SCS specimen. Consequently, the deformation of the SCS specimen was solely confined to the gage section. The microstructure of the undeformed region for sample A is shown in Fig. 2(a), which reveals wavy slip lines due to prior deformation by cold drawing. This microstructure is typical of regions a and c, for both the samples A and B.

The orientation of the grains in the undeformed section is shown by the (1 1 1) pole figure (Fig. 2(b)). The majority of the grains are oriented with their <1 1 1> axis parallel to the sample z_0 direction (i.e. the drawing direction), with a smaller number of grains having their <1 0 0> axis parallel to the sample z_0 direction. This texture matches with the well-known texture observed for wire drawn copper samples [8]. The texture was found

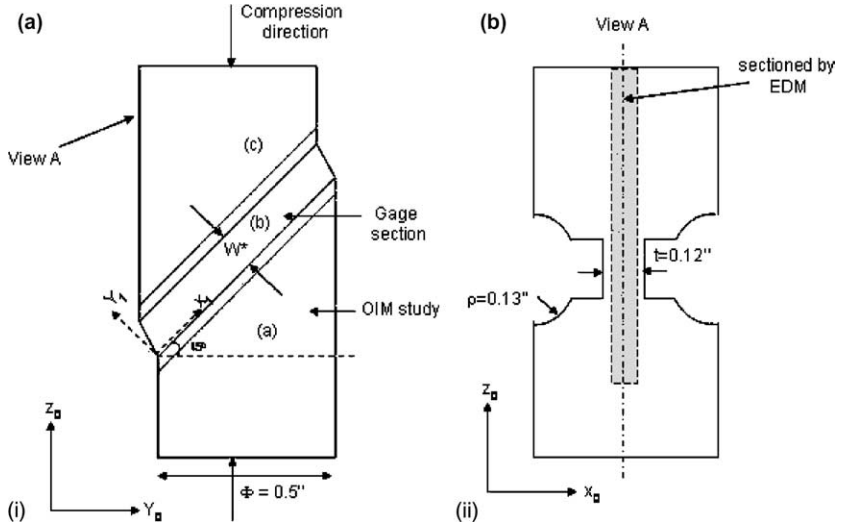

Fig. 1. Schematic showing the deformed SCS specimen. The diameter (Φ), thickness (t) and the clearance (ρ) were the same for both the samples studied in this case. OIM scans were carried out in the undeformed regions (a and c) and in the mid-section of the deformed region (b) for the samples A (quasi-static) and B (high strain rate).

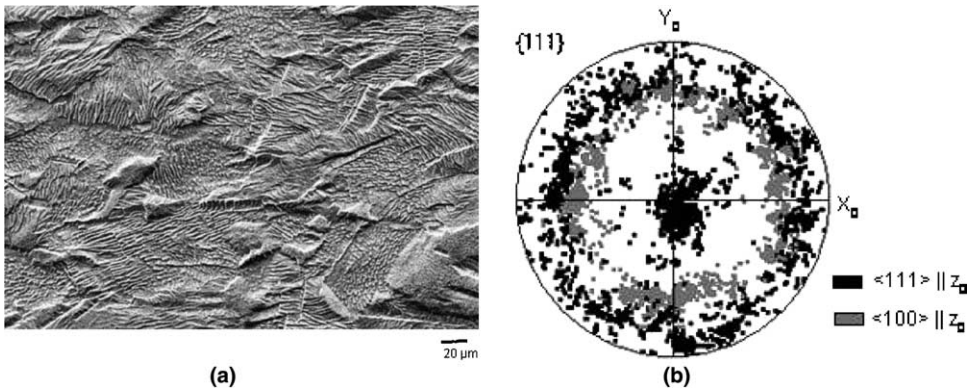

Fig. 2. (a) Microstructure of the undeformed region for sample A. (b) The texture in the undeformed region showing a combination of strong <1 1 1> fiber texture and weak <1 0 0> fiber texture.

to be uniformly the same in regions a and c for both the samples A and B after deformation.

3.1. Quasi-static deformation

The stress–strain curve for sample A deformed quasi-statically at a strain rate of 0.001 s^{-1} is shown in Fig. 3(a). The microstructure of the mid-region of the sheared region in sample A (i.e. region b) is shown in Fig. 3(b). Due to shear, the elongated grains appear to move away from the sample z_0 direction. The (1 1 1) pole figure from the same region is shown in Fig. 3(c). The pole figure is symmetrical about the y-axis which is commensurate with the sample symmetry. For better understanding, the axes are rotated to represent the pole figure in the "gage section (shear) co-ordinate system ($x_1 - y_1$)", as shown in Fig. 1. This pole figure (Fig. 3(d)) is similar to the known (1 1 1) pole figure obtained from torsion experiments. (Torsion experiments introduce simple shear as is the case in the present experiments which introduce shear dominant deformation in the gage section [9].)

3.2. Dynamic deformation

The stress–strain curve for sample B deformed dynamically at a strain rate of 7000/s is shown in Fig. 4(a). The microstructure of the mid-region of the

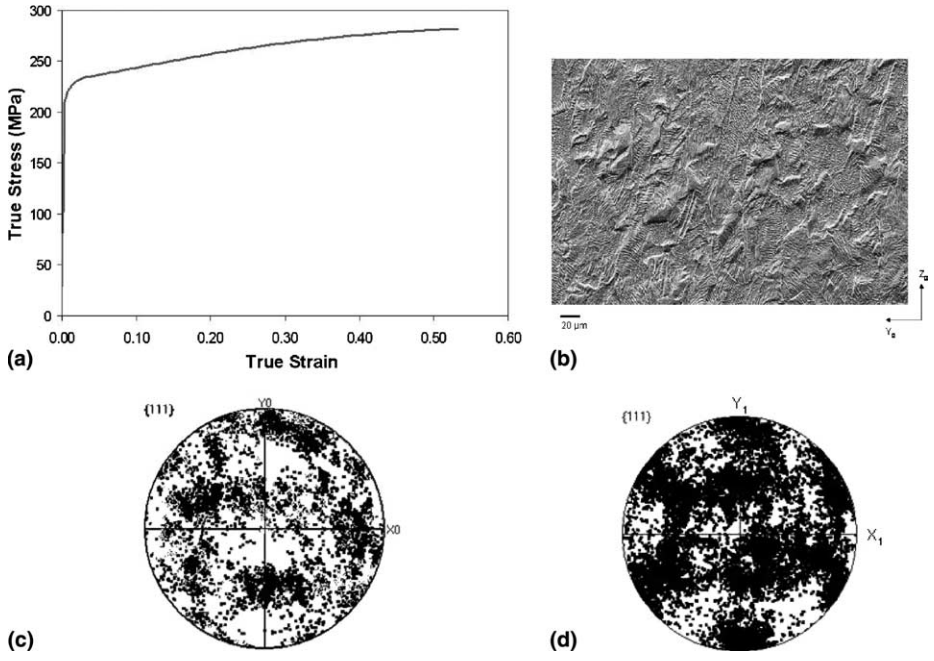

Fig. 3. (a) Equivalent stress–strain curve for sample A deformed at a strain rate of 10^{-3} s^{-1}, plotted from the experimental load displacement curve (P–d) using Eqs. (1) and (2). (b) Microstructure of the mid-region of the sheared region for the quasi-statically deformed sample A. (c) The texture in the mid-section of the deformed region for sample A. (d) The rotated texture in the gage section (shear) coordinate system (shown in Fig. 1) for sample A.

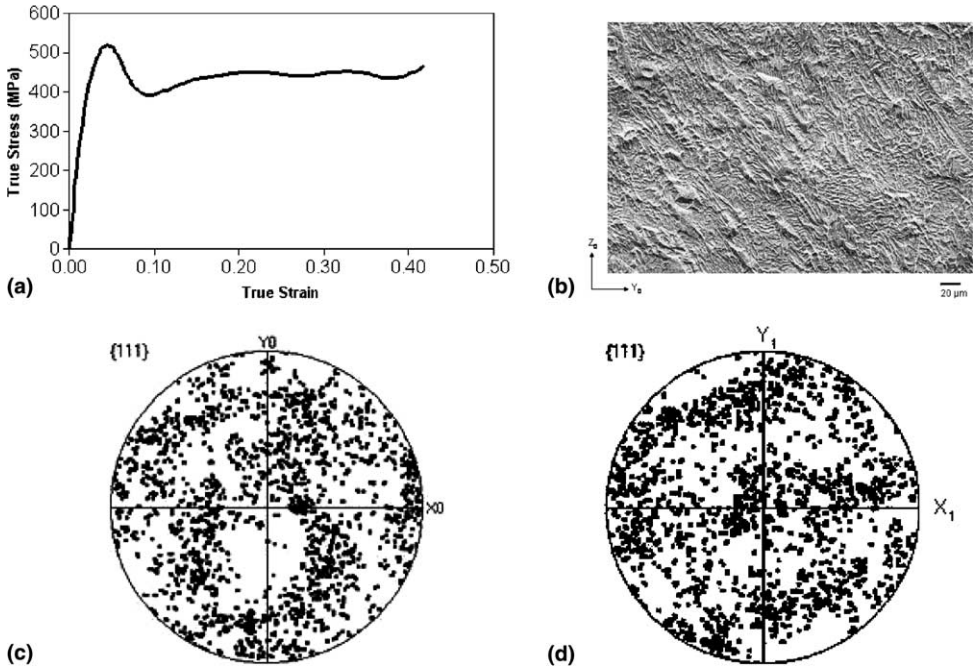

Fig. 4. (a) Equivalent stress–strain curve for sample B deformed at a strain rate of 7000 s^{-1} (the initial jump in stress is due to the non-equilibrium of the stress state along the length of the SCS observed generally during high strain rate testing with a split-Hopkinson bar). (b) Microstructure of the mid-region of the sheared region for the dynamically deformed sample B. (c) The texture in the mid-section of the deformed region for sample B. (d) The rotated texture in the gage section (shear) coordinate system for sample B.

sheared region in the dynamically deformed sample B (i.e. region b) is shown in Fig. 4(b). The corresponding pole figure from the mid-section of the sheared region is shown in Fig. 4(c) and (d).

Here, a major observation is that the two OFHC copper samples show different textures (Figs. 3 and 4) after deformation at different strain rate levels to the same equivalent strain.

This difference is not due to any recrystallization effects as recrystallization is only observed at very high strain rates of the order of 20,000 s^{-1} [3]. Moreover, the deformed microstructure (Fig. 4(a)) showed no evidence of recrystallized grains.

It is known from the torsion experiments that the grains rotate so that their <1 1 0> axis is along the shear direction [9]. Here, since the gage section experiences shear dominated deformation, a comparative study is conducted between the above two deformation textures (Figs. 3 and 4) to find the fraction of the grains that rotate accordingly. From the OIM maps generated during the scans for regions a, b and c, a fraction of the grains were found which had their <1 1 0> axes lying within 15° (selected arbitrarily) to the shear direction, x_1. Such fractions were obtained from all the three regions for both samples and converted into a histogram plot shown in Fig. 5. In order to visualize the effect of deformation on grain rotation, it may be assumed that the histogram plot for the undeformed region (regions a and c) is the same as that for the deformed region (region b) before the deformation, for both the samples. As expected, after deformation there is an increase in the fraction of the grains which have their <1 1 0> axis towards the shear direction, for both the samples A and B. However, the increase is larger for the low strain rate deformed sample A as compared to the high strain rate deformed sample B. Additionally, the effect of other components (i.e. <1 1 1> and <1 0 0> fiber textures) on

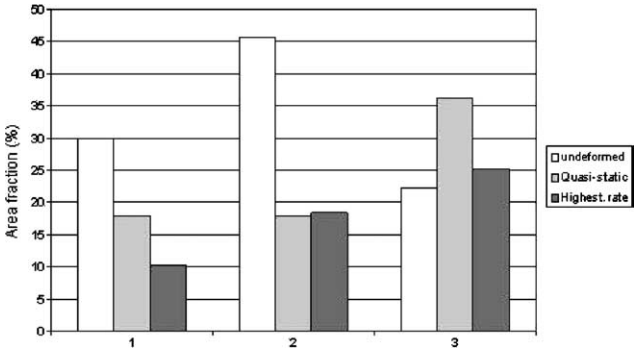

Fig. 5. Comparison chart showing the fraction of the grains with various major texture components found in the quasi-statically deformed sample A and dynamically deformed sample B: (1) the fraction of the grains having an orientation with their <1 0 0> axis lying within 15° to the sample z axis; (2) the fraction of the grains having an orientation with their <1 1 1> axis lying within 15° to the sample z axis; and (3) the fraction of the grains having an orientation with their <1 1 0> axis lying within 15° to x_1 axis (rotated frame), i.e. shear direction.

the shear dominated deformation is also plotted in Fig. 5. We observe that there is a significant decrease in the major component, after the deformation, for the two samples A and B.

3.3. On the uniformity of deformation

In order to check the uniformity of the textures, OIM scans were performed along the mid-section of the gage region for both the quasi-static and dynamically deformed samples and it was observed that the textures remained the same along the gage length. This feature indicates that the deformation was uniform in the SCS gage section as was numerically validated in earlier work [3].

4. Discussion

The present study characterizes the influence of strain rate on the deformation texture of as-received OFHC copper at room temperature. From the pole figures (Figs. 3(b) and 4(b)) it is observed that qualitatively different textures are obtained at widely different strain rates (deformed to the same strain level) thereby indicating the importance of strain rate on deformation texture. Further, from the grain rotation analysis (Fig. 5), it is found that there is a larger increase in the fraction of the grains that rotate to bring their <1 1 0> axis close to the shear direction (x_1) for the low strain rate sample as compared to the high strain rate sample. This suggests that the grains in the high strain rate deformed sample were inhibited from rotating towards the shear direction as compared to the low strain rate deformed sample. This effect maybe most likely due to higher initial strain hardening for the high strain rate deformed sample B as is seen by comparing the stress–strain curves (Figs. 3(a) and 4(a)). The apparently increased initial strain hardening at higher strain rate for copper has also been observed by other groups [10,11].

It may be important to note that similar experiments on body-centered cubic Ta revealed very less observable change in the deformation texture at a higher strain rate, which also maybe due to the fact that there is no increase in initial strain hardening at the higher strain rate [12]. Therefore, the observed difference in texture seem to directly related to strain hardening that is a function of the strain rate in itself. At a crystal level, this difference could be due to the difference in single-slip hardening on individual slip systems and/or due to the difference in latent hardening (or cross slipping, as concluded in Ref. [5]). However, the response of individual slip systems to variations in strain rate has not been extensively characterized for this material in order to verify the extent to which the resulting texture is affected by the strain rate. Consequently, single crystal studies are currently underway in order to explore these possibilities.

From our present experimental study we conclude that there is a need to develop an analytical expression (to be included in the constitutive equations) showing the dependency of strain hardening on strain rate for fcc metals.

5. Conclusion

The effect of strain rate on the deformation texture of polycrystalline OFHC copper has been investigated by means OIM. At higher strain rates, the material strain hardens thereby affecting the amount of crystal rotation and hence the texture. For copper the texture is strongly rate dependent. This result indicates the need for developing the current constitutive models for fcc metals in order to predict texture evolution during high strain rate dynamic processes.

Acknowledgement

The support of the Department of Energy through the Center for Dynamic Response of Materials at the California Institute of Technology is gratefully acknowledged. D.R. acknowledges the Fund for Promotion of research at Technion.

References

[1] Asaro RJ, Needleman A. Acta Metall 1985;33:923.
[2] Kalidindi SR, Bronkhorst CA, Anand L. J Mech Phys Solids 1992;40:537.
[3] Rittel D, Ravichandran G, Lee S. Mech Mater 2002;34:627.
[4] Leffers T. Scripta Metall 1968;2:447.
[5] Leffers T, Pedersen OB. Scripta Metall 2002;46:741.
[6] Adams BL, Kunze K, Wright SI. Metall Trans A 1993;24A:819.
[7] Wright SI. J Comp-Assisted Microsc 1993;5:207.
[8] English AT, Chin GY. Acta Metall 1965;13:1013.
[9] Kocks UF, Tome' CN, Wenk H-R. Texture and Anisotropy. Cambridge: Cambridge University Press; 1998. p. 87.
[10] Clifton RJ. Appl Mech Rev 1990;43:S9.
[11] Bodner SR, Rubin MB. J Appl Phys 1994;76:2742.
[12] Schoenfeld SE. Int J Plasticity 1998;14:871.